# Neutralized Ion Beam Spectroscopy

GREGORY I. GELLENE and RICHARD F. PORTER*

*Baker Laboratory of Chemistry, Cornell University, Ithaca, New York 14853*

*Received October 21, 1982 (Revised Manuscript Received January 20, 1983)*

Research on the neutralization of ion beams by electron-capture collisions with atomic particles has largely been within the domain of atomic and high-energy physics with the emphasis on understanding the fundamentals of ion–atom interactions. In this Account we present a chemist's perception of the possibilities to obtain new information about molecules formed by neutralization of beams of molecular ions. We will not deal with interactions involving atomic ions or with specific aspects of collisional activation or excitation of ions but only those reactions in which a molecule is formed in an electron-capture process.

Neutralized ion beam spectroscopy is defined in this Account as a technique for investigating modes of energy disposal in species formed when a fast beam of ions is neutralized in the electron-transfer reaction

$$AB^+ + M(g) \rightarrow AB^* + M^{+\ddagger} \qquad (1)$$

where $AB^+$ is any diatomic or polyatomic ion and M is a thermalized target atom. The state of AB produced in reaction 1 is dependent on the ionization potential of the target. The target atom series M = Cs, K, Na, Ca, Mg, and Zn that covers an ionization potential range of 3.9–9.4 eV will be considered. The technique we will describe is conceptually quite simple but is capable of providing information about a variety of unusual chemical species that would be difficult to prepare or study by more conventional techniques. We will discuss four applications, each illustrating a different aspect of the technique.

In principle any positively charged ion that can be produced in a mass spectrometer can be used as a projectile in reaction 1, allowing for the production of unstable or highly reactive neutrals under beam conditions. The apparatus employed in our laboratory has been extensively described elsewhere[1] and will only be mentioned briefly here. An ion beam, produced by electron impact or chemical ionization, is accelerated through 3–6 keV, mass resolved, and focused into a collision chamber containing a low pressure of metal-atom vapor (typically 1–5 mtorr). Unreacted ions egressing from the chamber are swept out of the beam by electrostatic deflection so only neutral species continue in flight toward the electron-multiplier detector. Translation of the detector normal to the beam axis samples beam intensity as a function of scattering angle ($I(\theta)$), giving rise to a neutral beam profile ($I(\theta)$ vs. $\theta$).

Under these experimental conditions the transit time required for a neutral to reach the detector is between about $10^{-7}$ and $10^{-6}$ s. If an excited neutral survives for a period longer than $10^{-6}$ s or radiatively decays to a stable state on a time scale shorter than $10^{-7}$ s (characteristic of allowed electronic transitions), then the full width at half-maximum (FWHM) of its beam profile will be essentially the same as that of the primary ion beam (Figure 1A, profile A). Alternatively, a neutral that dissociates on a time scale shorter than $10^{-7}$ s will give rise to a broadened profile due to the components of the fragment's velocity normal to the beam axis (Figure 1A, profile B). A combination of these events will give rise to a composite profile (Figure 1A, profiles C and D) as will a single dissociation process occurring on a time scale between $10^{-6}$ and $10^{-7}$ s (metastable species). For a profile of type C in Figure 1A it is generally possible to separate contributions of the stable and dissociative components to obtain branching ratios. It is important to note that some prior knowledge of the characteristics of the species is generally necessary in order to interpret its beam profile. When a neutral undergoes dissociation, as evidenced by beam broadening, the laws of conservation of energy and momentum allow the calculation of the fragmentation energy (the kinetic energy released by dissociation) by the relation

$$FE = -\frac{1}{2}M_1\left(1 + \frac{M_1}{M_2}\right)(V_{cm}\sin\theta_{max})^2 \qquad (2)$$

where $M_1$ is the mass of the fragment observed at the maximum laboratory scattering angle, $\theta_{max}$, $M_2$ is the mass of the other fragment, and $V_{cm}$ is the center of mass velocity.[2] Use of eq 2 requires a knowledge of the fragment masses (i.e., the dissociation pathway), which can be uniquely determined if $I(\theta)$ for both masses is observed. Since the efficiency of electron-multiplier detectors depends on the kinetic energy of the impacting particles, it is possible to distinguish profiles from heavy and light fragments if there is a substantial difference in their mass. By increasing the kinetic energy of the ion by postacceleration at the collision chamber, the light fragment (H or D) can be brought into detection. A potential advantage of detecting the light fragment is increased resolution because, for a fixed dissociation energy, the light fragment ($M_l$) scatters to higher angle ($\theta_l$) according to the relation

$$\left(\frac{\partial\theta_l}{\partial\theta_h}\right)_E = \frac{M_h}{M_l}\frac{\cos\theta_h}{\cos\theta_l} \approx \frac{M_h}{M_l} \qquad (3)$$

which is valid for small scattering angles.

Gregory Gellene is a graduate student in the Cornell Chemistry Department. He received his B.S. degree from Georgetown University in 1979. He is presently holder of a Proctor & Gamble Fellowship.

Richard Porter was born in Fargo, ND, in 1928. He received his B.S. degree from Marquette University and his Ph.D. in Chemistry from the University of California at Berkeley, where he studied with Leo Brewer. He spent a year in postdoctoral studies with Mark Inghram in the physics department of the University of Chicago, where he became interested in the use of mass spectrometry to investigate chemical species at high temperatures. He has been at Cornell since 1955 and is now Professor of Chemistry.

(1) G. I. Gellene, D. A. Cleary, and R. F. Porter, *J. Chem. Phys.*, 77, 3471 (1982).

(2) M. A. D. Fluendy and K. P. Lacoley, "Chemical Applications of Molecular Beam Scattering", Chapman and Hall, London, 1973, pp 37–43.

0001-4842/83/0116-0200$01.50/0 

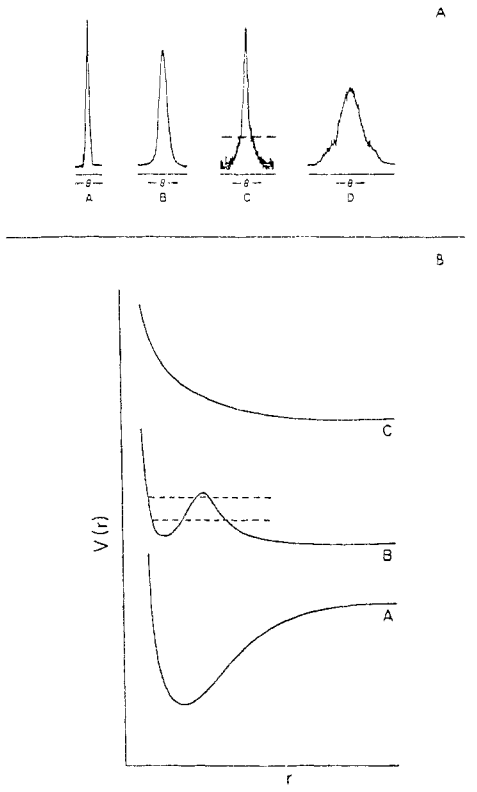


**Figure 1.** (A) Representative neutralized ion beam profiles. Profile A: stable neutral state. Profile B: dissociative neutral state. Profile C: composite of stable and dissociative states. The dotted line indicates how the profile is divided to determine the branching ratio. The integrated area above or below the dotted line is proportional to the amount of stable or dissociative state produced, respectively. Profile D: composite of two dissociative states. (B) Simple one-dimensional potential functions ($r$ = separation coordinate) associated with stable (potential A), metastable (potential B), and dissociative (potential C) states.

Figure 1B shows schematically three simple potential functions that may be used to describe the qualitative features of a single dissociation coordinate for a neutral species. In our observations potential of form A will manifest itself by a sharp beam profile with a FWHM similar to that of the precursor ion beam, while potential of form C will give rise to a smooth dissociation continuum (generally structureless). The presence of a predissociation barrier (potential B) can be inferred from structural features in the beam profile resulting from dissociation of the quantized states lying below the barrier. In some cases these internal states can be identified by the higher resolution achieved in the beam profile of the light fragment. Structure in the light-particle profile may also result if the heavy particle is formed in excited vibrational states. This structure will appear below $\theta_{max}$.

## Excited Products Exhibiting Radiative Emission

When an ion captures an electron to an excited state of the neutral (AB*) with a sufficiently long dissociation lifetime, or leaves behind an excited target ion ($M^{+*}$), a radiative process may occur. Some of the electron-transfer reactions, $AB^+/M$, from which radiative emission has been observed are $He_2^+/(N_2, CO, O_2, NO,$[3] Cd,[4] Mg, Zn,[5] Li[6]), $Ne_2^+/(N_2, CO, CO_2$[7]), $N_2^+/$(Na, K,

(3) G. H. Bearman, J. D. Earl, R. J. Pieper, H. H. Harris, and J. J. Leventhal, *Phys. Rev. A*, **13**, 1734 (1976).

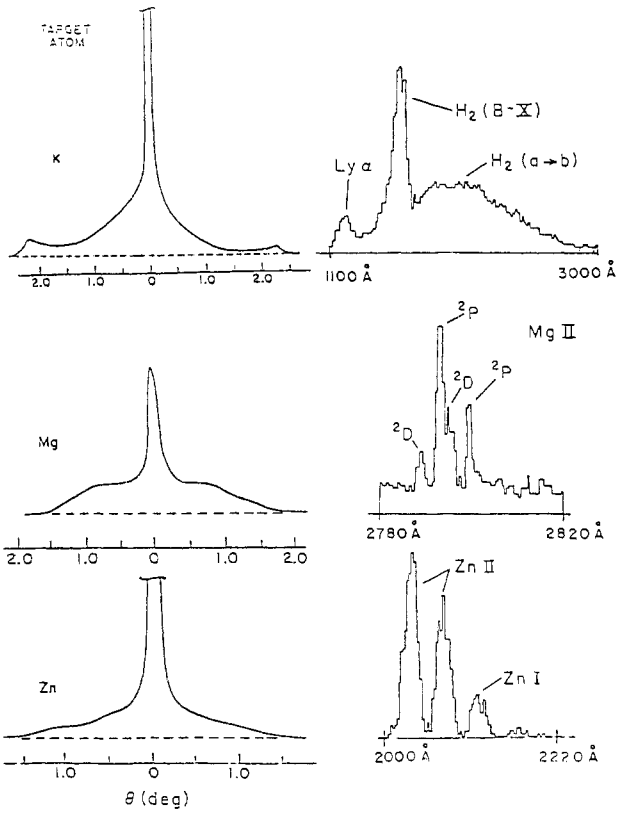


**Figure 2.** Neutralized ion beam profiles (left column) and optical emission spectra (right column) observed following the electron-transfer reaction between $H_2^+$ and M.

Li,[8] He[9]), $H_2^+/(N_2O$,[10] Li[6]), $H_3^+/N_2O$,[10] and $CO^{2+}/H_2$.[11] Reference 12 describes a combied optical-spectroscopy and beam-scattering study of the reaction

$$H_2^+ + M(g) \rightarrow H_2^* + M^{+*} \quad (4)$$

where M = Cs, K, Mg, and Zn. The well-characterized bound and dissociative electronic states of $H_2$ make the $H_2^+/M$ system a particularly good one for a detailed investigation by the combined techniques, and a major conclusion of that work is that reaction 4 occurs under near resonant conditions with vertical transitions in the range of ion velocities studied ($3–7 \times 10^7$ cm/s). Tal'rose et al. measured cross sections of approximately 25–75 Å$^2$ for reaction 4 where M = K, Li, Mg, Zn.[13]

Figure 2 shows neutral beam profiles and optical emission spectra obtained following reaction 4 when the target atom was K, Mg, and Zn. The profiles obtained for these target metals exhibit a composite nature, indicating the formation of both a stable and dissociative state of $H_2$ in each case (typical of Figure 1, profile C). The observed optical spectra for the three systems,

(4) F. Ranjbar, H. H. Harris, and J. J. Leventhal, *Appl. Phys. Lett.*, **31**, 385 (1977).
(5) G. D. Myers and J. J. Leventhal, *Phys. Rev. A*, **18**, 434 (1978).
(6) G. D. Myers, J. L. Barrett, and J. J. Leventhal, *Phys. Rev. A*, **20**, 797 (1979).
(7) G. H. Bearman, J. D. Earl, H. H. Harris, and J. J. Leventhal, *Appl. Phys. Lett.*, **29**, 108 (1976).
(8) J. L. Barrett and J. J. Leventhal, *J. Chem. Phys.*, **71**, 4015 (1979).
(9) J. D. Kelly, G. H. Bearman, H. H. Harris, and J. J. Leventhal, *Chem. Phys. Lett.*, **50**, 295 (1977).
(10) G. H. Bearman, H. H. Harris, and J. J. Leventhal, *J. Chem. Phys.*, **66**, 4111 (1977).
(11) G. H. Bearman, F. Ranjbar, H. H. Harris, and J. J. Leventhal, *Chem. Phys. Lett.*, **42**, 335 (1976).
(12) G. I. Gellene, D. A. Cleary, R. F. Porter, C. E. Burkhardt, and J. J. Leventhal, *J. Chem. Phys.*, **77**, 1354 (1982).
(13) N. V. Kir'yakov, M. I. Markin, and V. L. Tal'roze, *Dokl. Phys. Chem. (Engl. Transl.)*, **260**, 892 (1982).

Table I
Summary of Analysis of Beam Profiles and Optical Spectra Obtained from $H_2^+$/M Reaction Products

| target atom | source conditions | neutralization products | FE, eV | branching fraction |
|---|---|---|---|---|
| K | $H_2$ | $K^+(3p^6,{}^1S) + H_2(a^3\Sigma_g^+) \xrightarrow{h\nu} H_2(b^3\Sigma_u^+) \rightarrow 2H(1s,{}^2S)$ | −1.45 | 0.64 |
| | | $K^+(3p^6,{}^1S) + H_2(b^3\Sigma_u^+) \rightarrow 2H(1s,{}^2S)$ | −6.72 | |
| | | $K^+(3p^6,{}^1S) + H_2(B^1\Sigma_u^+) \xrightarrow{h\nu} H_2(X^1\Sigma_g^+)$ | 0.0 | 0.36 |
| | $H_2$/He | $K^+(3p^6,{}^1S) + H_2(a^3\Sigma_g^+) \xrightarrow{h\nu} H_2(b^3\Sigma_u^+) \rightarrow 2H(1s,{}^2S)$ | −3.06 | 0.46 |
| | | $K^+(3p^6,{}^1S) + H_2(B^1\Sigma_u^+) \xrightarrow{h\nu} H_2(X^1\Sigma_g^+)$ | 0.0 | 0.54 |
| Mg | $H_2$/He | $Mg^+(3s,{}^2S) + H_2(b^3\Sigma_u^+) \rightarrow 2H(1s,{}^2S)$ | −4.02 | 0.81 |
| | | $H_2(X^1\Sigma_g^+) + Mg^+(3d,{}^2D) \xrightarrow{h\nu} Mg^+(3p,{}^2P) \xrightarrow{h\nu} Mg^+(3s,{}^2S)$ | 0.0 | 0.13 |
| | | $H_2(X^1\Sigma_g^+, v'' = n) + Mg^+(3p,{}^2P) \xrightarrow{h\nu} Mg^+(3s,{}^2S)$ | 0.0 | 0.06 |
| Zn | $H_2$ | $Zn^+(4s,{}^2S) + H_2(b^3\Sigma_u^+) \rightarrow 2H(1s,{}^2S)$ | −2.97 | 0.58 |
| | | $H_2(X^1\Sigma_g^+) + Zn^+(4p,{}^2P) \xrightarrow{h\nu} Zn^+(4s,{}^2S)$ | 0.0 | 0.42 |
| | $H_2$/He | $H_2(X^1\Sigma_g^+) + Zn^+(4p,{}^2P) \xrightarrow{h\nu} Zn^+(4s,{}^2S)$ | 0.0 | ~1.0 |

however, are very different with radiative processes involving different products of reaction. The B → X singlet and a → b triplet transition of $H_2$ occurs when K is the target, while these transitions are absent with Zn and Mg targets. These results indicate that with K targets the direct products of reaction 4 are the excited $B^1\Sigma_u^+$ and $a^3\Sigma_g^+$ states of $H_2$, which radiate to the lowest singlet ($X^1\Sigma_g^+$) and triplet ($b^3\Sigma_u^+$) states of $H_2$, respectively. These effects appear as the stable and dissociative components of the beam profile, respectively. In addition the beam profiles obtained with K targets show a scattering feature at $\theta \sim 2°$, which corresponds to a fragmentation energy of approximately −6.7 eV. An energy balance argument indicates that this feature cannot result from a radiative transition from the $a^3\Sigma_g^+$ state[14] but is due to nonradiative electron capture to the $b^3\Sigma_u^+$ state. A similar feature in the kinetic energy range of 7.2–10.4 eV was observed under high resolution by Meierjohann and Vogler[15] using $H_2$ as the target. They interpreted this as resulting from the nonresonant formation of the $C^3\pi_u$ state of $H_2$, which predissociates into the repulsive $b^3\Sigma_u^+$ state. Since we do not observe scattering at angles corresponding to a kinetic energy of 7.2–10.4 eV and predissociation of the $C^3\pi_u$ state would release a minimum of about 7.2 eV, it appears unlikely that the scattering features in the two experiments are the same.

When the target is Zn atoms, the only radiative process observed from the products of the reaction is the $4p,{}^2P \rightarrow 4s,{}^2S$ transition (approximately 6 eV) of $Zn^+$ and no hydrogen emission is observed. These results indicate that the lowest singlet and triplet states of $H_2$ again give rise to the stable and dissociative components of the beam profile, respectively, but in this case they are the direct products of reaction 4. Energy-resonance arguments (Figure 3) indicate that production of the excited 4p, $^2P$ state of $Zn^+$ should be associated with $H_2(X^1\Sigma_g^+)$ formation, while production of ground-state $Zn^+$ should be associated with $H_2(b^3\Sigma_u^+)$ formation.

Ionization by electron impact will, in general, produce ions in various degrees of excitation and it is well-known that this occurs for hydrogen.[16] The amount of internal

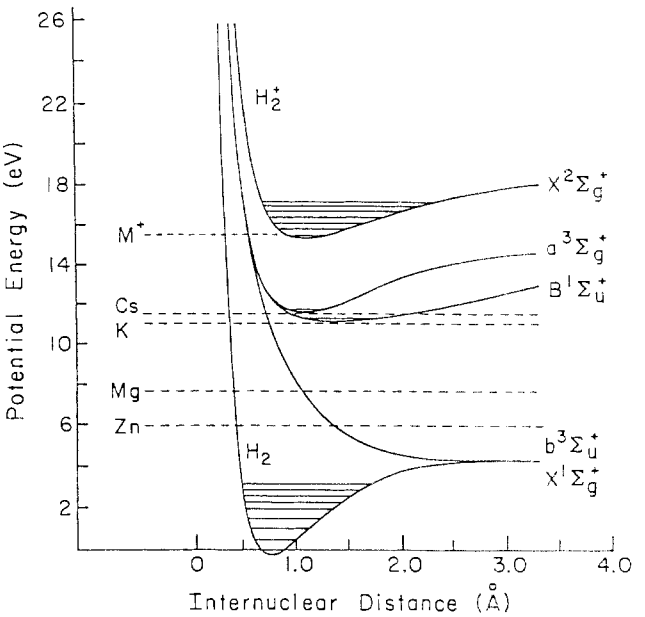


**Figure 3.** Potential energy curves for electronic states of $H_2^+$ and $H_2$ relevant to this discussion. Dashed lines indicate ground-state levels of metal atoms scaled with respect to their ionization potentials. These dashed lines intersect potential curves at $H_2$ internuclear distances corresponding to hypothetical resonant electronic capture configurations with respect to $H_2^+(X^2\Sigma g^+, v' = 0)$.

energy in the $H_2^+$ ion can be reduced by addition of a buffer gas to the ion source, and the product distribution in the $H_2^+$/M system was observed to depend on the vibrational excitation of the $H_2^+$ ions (Table I). Quenching of the $H_2^+$ by collisions with He had the effect of diminishing both the scattering feature at $\theta \sim 2°$ observed with K targets and the dissociative component of the beam profile observed with Zn targets. These results can be understood in terms of the electron-transfer process occurring vertically. Figure 3 shows that direct resonant electron transfer from K to the $b^3\Sigma_u^+$ state of $H_2$ will occur vertically with high probability only from the left-hand "turning point" of vibrationally excited $H_2^+$, while electron transfer from Zn to the $b^3\Sigma_u^+$ state of $H_2$ will occur vertically only

(14) G. Herzberg, "Spectra of Diatomic Molecules", Van Nonstrand-Reinhold, Princeton, NJ, 1950.
(15) B. Meierjohann and M. Vogler, *Phys. Rev. A*, 17, 47 (1978).
(16) J. Berkowitz and R. Spohr, *J. Electron Spectrosc. Relat. Phenom.*, 2, 143 (1973).

Table II
Energy Levels ($E_{AB^*}$) and Electron Affinities ($EA_{AB^*}$) Determined by Neutralized Ion Beam Spectroscopy[a]

| AB* | target atom | dissoc pathway | $E_{AB^*}$[b] | lit. value[c] | $EA_{AB^*}$ | lit. value[c] |
|---|---|---|---|---|---|---|
| $H_3$(gs) | Mg | $H_3 \rightarrow H_2 + H$ | 2.2 | (2.49)[e] | 7.0 | |
| $CH_5$(gs) | Na | $CH_5 \rightarrow CH_4 + H$ | 2.65 | | 5.3 | (8.3)[f] |
| $CH_4(^3T_2)$ | Na | $CH_4 \rightarrow CH_3 + H$ | 7.60 | 7.5[g] | 5.18 | |
| $CH_3(^2A'_1)$ | K | $CH_3 \rightarrow CH_2(^1A'_1) + H$ | 5.99 | 5.73[h] | 3.85 | |
| $CH_2(^3A_1)$ | K | $CH_2 \rightarrow CH + H$ | 6.42 | (6.37)[i] | 3.98 | |
| $CH(^2\Sigma^+)$ | Na | $CH \rightarrow C(^1D) + H$ | 5.30 | 4.0-5.5[j] | 5.34 | |
| $H_3O$(gs) | Na | $H_3O \rightarrow H_2O + H$ | 1.12 | (2.12)[f] | 5.3 | (4.70)[k] |
| $H_3S$(gs) | Na | $H_3S \rightarrow H_2S + H$ | 1.03 | | 4.9 | (6.0-6.5)[l] |
| $NH_4$(gs) | Na | $NH_4 \rightarrow NH_3 + H$ | 0.10 | | 4.73[d] | (3.8-4.8)[m] |
| $PH_4$(gs) | Na | $PH_4 \rightarrow PH_3 + H$ | 0.45 | | 4.86 | (5.0-6.0)[l] |
| HCNH(gs) | Na | $HCNH \rightarrow HCN + H$ | 1.8 | (<1.2)[n] | 4.0 | |
| $C_2H_5$(bridged) | Ca | $C_2H_5 \rightarrow C_2H_4 + H$ | 0.5 | (0.3-0.9)[o] | 6.2 | |

[a] All values are in electron volts; gs = ground electronic state. [b] $E_{AB^*} = -FE$ (unstable ground state), or $E_{AB^*}$ = excitation energy (stable ground state). [c] Values in parentheses are the result of theoretical calculations. [d] In this case the ionization potential is reported. [e] R. N. Porter, R. M. Stevens, and M. Karplus, *J. Chem. Phys.*, **49**, 5163 (1968); P. Siegbahn and B. Liu. *ibid.*, **68**, 2457 (1978). [f] See ref 32. [g] H. H. Brongersma and L. J. Oosterhoff, *Chem. Phys. Lett.*, **3**, 437 (1969). [h] G. Herzberg, *Proc. R. Soc. London, Ser. A*, **262**, 291 (1961). [i] J. Romelt, S. D. Peyreimhoff, and R. J. Buenker, *Chem. Phys.*, **54**, 147 (1981). [j] G. Herzberg and J. W. C. Johns, *Astrophys. J.*, **158**, 399 (1969); H. P. D. Lui and G. Verhaegen, *J. Chem. Phys.*, **53**, 735 (1970). [k] M. E. Schwartz, *Chem. Phys. Lett.*, **40**, 1 (1976). [l] W. H. E. Schwarz, *Chem. Phys.*, **11**, 217 (1975). [m] See ref 29-34. [n] M. S. Gorden and J. A. Pople, *J. Chem. Phys.*, **49**, 4643 (1968). [o] See ref 38.

from the right-hand "turning point" of vibrationally excited $H_2^+$. The effect of vibrational quenching of the $H_2^+$ ion on the $H_2(b^3\Sigma_u^+)$ produced by the radiative transition is an increase in FE (Table I). This can be understood in terms of an increased production of low vibrational states of $H_2(a^3\Sigma_g^+)$, leading to a red-shifting of the a → b transition.[17]

Electron transfer from Mg to $H_2^+$ is observed to produce two excited states of $Mg^+$ (the 3p,$^2$P and 3d,$^2$D states lying approximately 4.43 and 8.86 eV above the ground state of $Mg^+$, respectively) by the reactions

$$H_2^+(X^2\Sigma_g^+) + Mg(3s^2, {}^1S) \rightarrow H_2(X^1\Sigma_g^+, v'' \sim 0) + Mg^+(3d, {}^2D) \quad (5a)$$

$$H_2^+(X^2\Sigma_g^+) + Mg(3s^2, {}^1S) \rightarrow H_2(X^1\Sigma_g^+, v'' = 5\text{-}11) + Mg^+(3p, {}^2P) \quad (5b)$$

both of which are associated with favorable Franck–Condon factors.[18] Figure 3 indicates that reactions 5a and 5b will occur with high probability by vertical electron transfer from the left- and right-hand "turning points", respectively. It is interesting to note that a recent study of $H_2^+/(N_2, CO, O_2)$ also indicated the importance of energy resonance and Franck–Condon effects even at low collisional energies.[19]

## Neutrals Produced in Their Ground States

When a target atom has an ionization potential close to the electron affinity of the projectile ion, resonance electron capture will result in the formation of neutrals predominately in their ground states. For many small polyatomic ions this condition is satisfied with the target atom Zn (IP = 9.4 eV) as illustrated by the electron-transfer reaction

$$CH_n^+ + Zn(g) \rightarrow CH_n + Zn^+ \qquad n = 1\text{-}4 \quad (6)$$

which give rise to narrow neutral beam profiles (Figure 1A, profile A) characteristic of stable states.[20] While the ground states of these small hydrocarbon fragments have been characterized spectroscopically and their ground-state stabilities well-known, there are many ions for which the neutral is of unknown stability. Thus, this technique can be used to demonstrate the existence (or nonexistence) of neutrals with bound ground states. In addition, when a neutral is produced in a stable ground state, the technique provides a means of generating molecules in a collision-free beam of well-defined kinetic energy.

In a high-pressure ion source it is possible to generate ions such as $H_3^+$, $H_3O^+$, and $CH_5^+$, which lead to unstable molecules on neutralization.[21,22] A fragmentation energy can be calculated from beam profiles (typical of Figure 1A, profile B), providing a quantitative measure of the instability of the molecule. To our knowledge this is the first experimental measurement of $CH_5$. For systems where the energy of the ion ($E_{AB^+}$) can be determined from available thermochemical data, the fragmentation energy can be used in the relation

$$EA_{AB^+} = E_{AB^+} + FE - (E_A + E_B) \quad (7)$$

to determine the vertical electron affinity of the ion ($EA_{AB^+}$) when the neutral AB fragments to A + B. Table II summarizes vertical electron affinities for a number of ions determined by this procedure. It is possible that the structure of an ion may not be the same as that of the stable neutral. In this case vertical electron transfer may produce a neutral species in a state of excitation sufficient for dissociation. Beam measurements indicate a small fragmentation energy for $PH_4$; however, a long-lived neutral component was not observed. This probably reflects an ion/radical geometry change as the ion is generally believed to have a tetrahedral structure,[23] while there is ESR evidence indicating that the radical is at least metastable with

(17) H. M. James and A. S. Coolidge, *Phys. Rev.*, **55**, 184 (1939).
(18) R. W. Nicholls, *J. Phys. B*, 1, 1192 (1968).
(19) S. L. Anderson, T. Turner, B. H. Mahan, and Y. T. Lee, *J. Chem. Phys.* **77**, 1842 (1982).
(20) G. I. Gellene, B. W. Williams, and R. F. Porter, *J. Chem. Phys.*, **24**, 5636 (1981).
(21) P. M. Curtis, B. W. Williams, and R. F. Porter, *Chem. Phys. Lett.*, **65**, 296 (1979).
(22) B. W. Williams and R. F. Porter, *J. Chem. Phys.*, **73**, 5598 (1980).
(23) M. Krogh-Jespersen, J. Chandrasekhar, E. Würthwein, J. B. Collins, and P. von Ragué Schleyer, *J. Am. Chem. Soc.*, **102**, 2263 (1980).

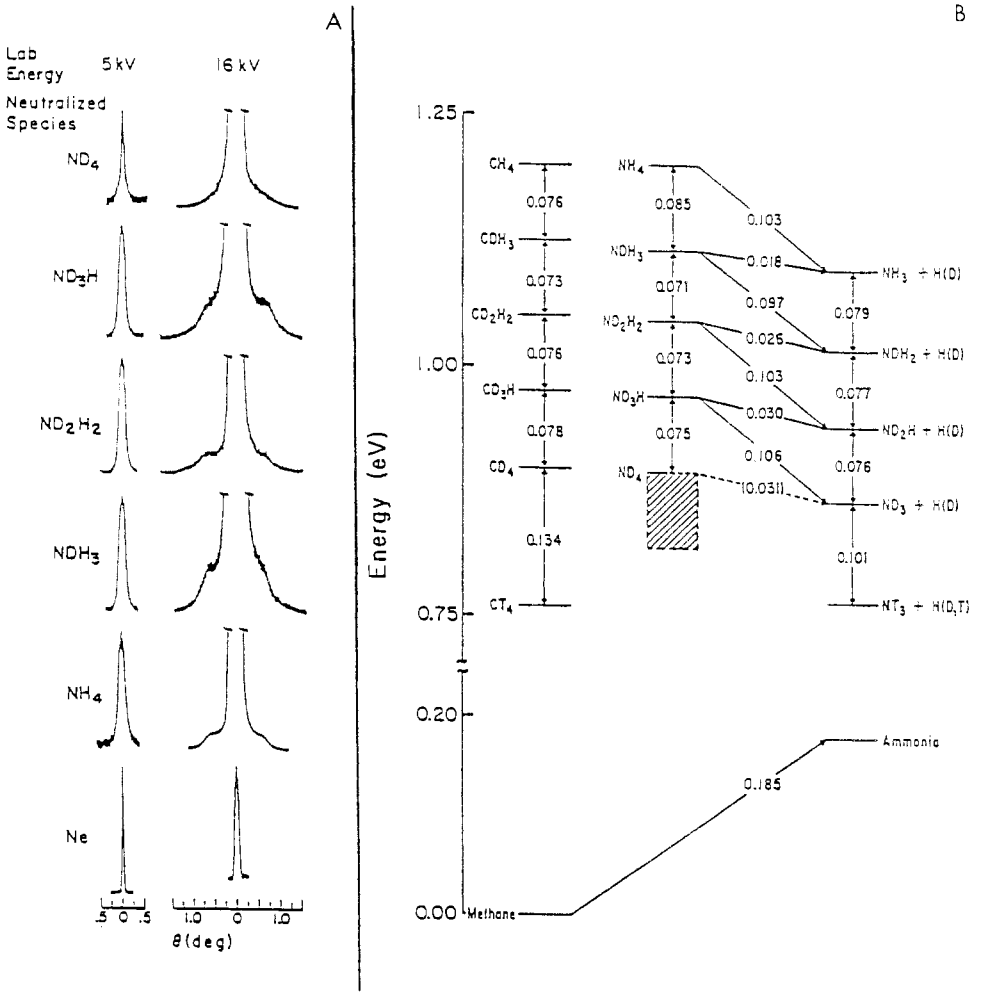


**Figure 4.** (A) neutralized ion beam profiles of heavy ($NH_3D_{3-n}$) and light (H, D) fragmentation products (left and right columns, respectively) observed following the electron-transfer reaction between $NH_4D_{4-n}^+$ and Na. (B) Energy scaling of isotopically substituted ammonium radicals with respect to their dissociation products.

a distorted trigonal-bypyramidal structure.[24]

The ammonium radical provides an interesting intermediate case of a molecule with a metastable ground state.[1] It is believed that both the ion and the radical have tetrahedral structures.[25] Neutral beam profiles resulting from the electron-transfer reaction

$$NH_nD_{4-n}^+ + Na \rightarrow NH_nD_{4-n} + Na^+ \quad n = 0\text{–}4 \qquad (8)$$

are shown in Figure 4A. At a laboratory energy of 5 kV only the heavy dissociation fragment (ammonia) is detected. The beam profiles shown in the first column of Figure 4A are similar for all species with one or more H atoms. Profiles obtained from fully deuterated radicals ($ND_4$), however, are composite in nature, indicating the existence of a long-lived stable and short-lived dissociative states. When the laboratory energy is increased to 16 kV, the light dissociation fragment is also detected (Figure 4A, column 2), and profiles obtained from hydrogen containing radicals exhibit a scattering feature at $\theta = 0.6\text{–}0.7°$ (FE $\approx -0.1$ eV) along with an underlying continuum. The center truncated region corresponds to the heavy ammonia fragment, which is detected at greater sensitivity under these conditions. In contrast, profiles obtained from $ND_4$ at these energies are structureless, exhibiting only the smooth fragmentation continuum with the sharp central spike from the heavy-fragment profile obscured in the truncated region. Agreement between fragmentation energies calculated from light- and heavy-fragment profiles indicate that loss of atomic hydrogen is the predominate dissociation process although loss of molecular hydrogen is thermodynamically allowed. The results of the energetic calculations are summarized in the energy-level diagram (Figure 4B), which shows the relative stability of the isotopically substituted ammonium radicals with respect to their dissociation products. Loss of deuterium atoms from isotopically mixed radicals, although energetically allowed, was not observed in these experiments. A preferential loss of H atoms is consistent with a tunneling dissociation mechanism involving a predissociation barrier. This conclusion is further substantiated by the observation of an undissociated state of $ND_4$. Whether the stability of $ND_4$ is thermodynamic or kinetic in nature is not presently known and the cross-hatched region of Figure 4B bounds the region where the zero point of $ND_4$ would be expected. From the zero-point dissociation energy of $NH_4$ eq 7 can be used to determine the ionization potential of the radical rather than the vertical electron affinity.[26] If

(24) A. J. Colussi, J. R. Morton, and K. F. Preston, *J. Chem. Phys.*, **62**, 2004 (1975).
(25) E. Broclawik, J. Mrozek, and V. H. Smith, Jr., *Chem. Phys.*, **66**, 417 (1982).
(26) Proton affinity of $NH_3$ was taken to be 8.76 ± 0.06 eV; S. T. Ceyer, P. W. Tiedemenn, B H. Mahan, and Y. T. Lee, *J. Chem. Phys.*, **70**, 14 (1979).

rotational energy is neglected, a value of 4.73 ± 0.06 eV is calculated.

Although emission spectra from excited Rydberg states of the ammonium radical have been observed,[27] until recently its ground-state stability has remained an open question. Much of the early literature has been summarized by Wan;[28] however, there does not appear to have been any previous definitive experimental work addressing the subject. There have been several theoretical calculations of the ionization potential of the radical, and with the exception of a recent $X\alpha$ value of 4.85 eV,[25] most of the results fall between 3.8 and 4.1 eV.[29-34] The discrepancy between our results and the calculated values seems to arise from a theoretical underestimation of the stability of the ground-state radicals. This would also cause predicted Rydberg transitions to be red-shifted.

The fragmentation energies arising from the dissociation of the continuum states can be used to estimate the height of the potential maximum in the dissociation coordinate of the ground state of the ammonium radical. The "top of the barrier" should lie approximately between the lowest continuum state and the highest quantized state observed.[1] This places the height of the barrier between 0.33 and 0.40 eV above the dissociation products of $ND_3$ and D. It remains an open question whether the radical would be stabilized in a condensed state since such a substance would be expected to have metallic properties.[28]

### Neutrals Produced in Excited Dissociative States

Use of metals of low ionization potential (Na, K, Cs) in reaction 1 generally results in electronically excited neutrals if the electron affinity of the projectile ion is several volts above the ionization potential of M. If the excited state is unstable and the molecule dissociates, its excitation energy ($E_{AB^*}$) can be determined from the calculated fragmentation energy and the relation

$$E_{AB^*} = E_A + E_B - E_{AB} - FE \tag{9}$$

where AB* dissociates to fragments A and B. Of particular significance is the ability of this technique to locate spin states of a molecule that are not accessible by optical transitions from the ground state. If the ionization potential of AB ($IP_{AB}$) is known, a vertical electron affinity for the excited state ($EA_{AB^*}$) can be calculated from the relation

$$EA_{AB^*} = IP_{AB} - E_{AB^*} \tag{10}$$

An example of this class of molecules is provided by the small hydrocarbon fragments ($CH_n$, $n$ = 2–4) produced by electron-transfer reactions of $CH_n^+$ and Na or K atoms.[20] Values of $E_{AB^*}$ and $EA_{AB^*}$ determined from $CH_n$ beam-profile measurements are summarized in Table II. The agreement of these values for $E_{AB^*}$ with previous literature values is an encouraging incentive to apply neutral beam techniques for investigation of excited electronic states of systems that are not yet well-characterized.

### Neutrals Produced from a Mixture of Ion Isomers

A composite neutralized ion beam profile (Figure 1A, profiles C and D) can arise in fundamentally two different ways: (case 1) a single ion species may branch into two neutral states or (case 2) two ionic species in the beam may each capture an electron, producing two neutral states. When two ion "isomers" are present they may differ either in their electronic structure (excited states that do not relax prior to neutralization) or in their geometric structure. Since, in general, the different isomers will be associated with different energies, beam profiles obtained with an appropriate target will also be different and can serve as "fingerprints" of the isomers. To distinguish case 1 from case 2, we conisider the following relationships. For case 1, the neutral beam intensity is described by the equations

$$(I_1 + I_2)/I^\circ = 1 - e^{-(\sigma_1 + \sigma_2)nl} \tag{11a}$$

and

$$(I_1/I_2) = \sigma_1/\sigma_2 \tag{11b}$$

where $I_1$ and $I_2$ are neutral beam itensities, $I^\circ$ is the total beam intensity (ions plus neutrals), $\sigma$ is the cross section for electron transfer, $n$ is the metal atom number density, and $l$ is the interactive path length.

For case 2, the analogous equations are

$$(I_1 + I_2)/I^\circ = \alpha(1 - e^{-\sigma_1 nl}) + (1 - \alpha)(1 - e^{-\sigma_2 nl}) \tag{12a}$$

and

$$\frac{I_1}{I_2} = \frac{\alpha}{(1-\alpha)} \frac{1 - e^{-\sigma_1 nl}}{1 - e^{-\sigma_2 nl}} \tag{12b}$$

where $\alpha$ is the fraction of ions reacting with cross section $\sigma_1$. At low target number density, eq 12b reduces to the approximate form

$$\frac{I_1}{I_2} = \frac{\alpha}{(1-\alpha)} \frac{\sigma_1}{\sigma_2}\left[1 + (\sigma_2 - \sigma_1)\frac{nl}{2}\right] \tag{12c}$$

Therefore, we can distinguish case 1 from case 2 by observing $I_1/I_2$ at low metal-atom densities.

### Geometric Isomers: $C_2H_5^+$

Beam profiles of the heavy dissociation fragment resulting from electron-transfer reactions between five metal targets and $C_2D_5^+$ ions are shown in Figure 5A. The composite nature of each profile (with the possible exception of those obtained with Ca targets) demonstrates that two processes are occurring in each case. With targets of low ionization potential (Na, K), the ethyl radicals are formed in two different dissociative states, while with metals of high ionization potential (Mg, Zn), one stable and one dissociative state is formed. With the metal of intermediate ionization potential (Ca), predominately a single dissociative state is produced. Beam profiles of the light fragment observed at higher ion kinetic energy indicates that the dissociative process is atomic hydrogen loss in all cases.

An increase in the dissociative/stable state ratio ($I_1/I_2$) was observed at low Mg-atom densities, indicating that two distinguishable ions are present in the

(27) G. Herzberg, *Faraday Discuss. Chem. Soc.*, **71**, 165 (1981).
(28) J. K. S. Wan, *J. Chem. Educ.*, **45**, 40 (1968).
(29) D. M. Bishop, *J. Chem. Phys.*, **40**, 432 (1964).
(30) C. E. Melton and H. W. Joy, *J. Chem. Phys.*, **48**, 5286 (1968).
(31) W. Strehl, H. Hartmann, K. Hensen, and W. Sarholz, *Theoret. Chem. Acta*, **18**, 290 (1970).
(32) W. A. Lathan, W. J. Hehre, L. A. Curtiss, and J. A. Pople, *J. Am. Chem. Soc.*, **93**, 6377 (1971).
(33) G. R. Wight and C. E. Brion, *Chem. Phys. Lett.*, **26**, 607 (1974).
(34) S. Raynor and D. R. Herschbach, *J. Phys. Chem.*, **86**, 3592 (1982).

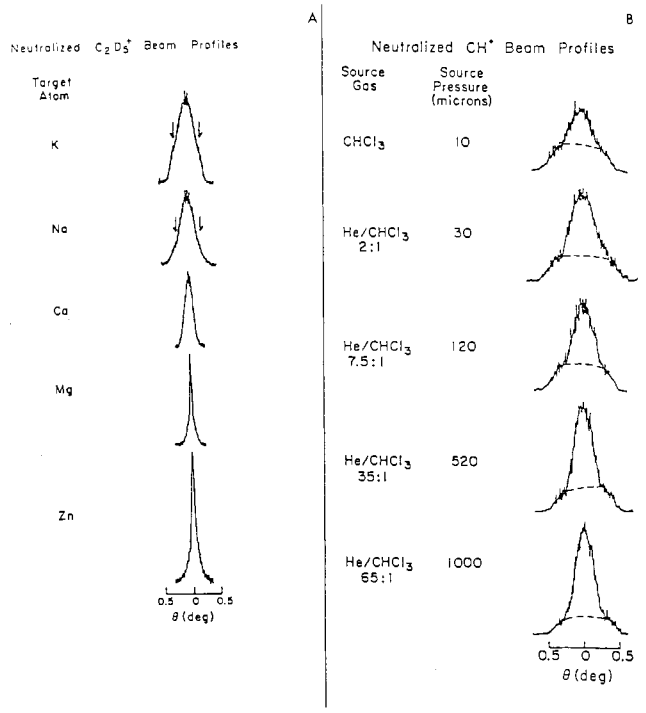


**Figure 5.** (A) Neutralized ion beam profiles observed following the electron-transfer reaction between $C_2D_5^+$ and M. The arrows designate the approximate location of the "break" in the profiles obtained with K or Na targets. This indicates the occurrence of two dissociative processes in these cases. (B) Neutralized ion beam profiles observed following the electron-transfer reaction between $CH^+$ and K as a function of He ion source pressure. The two portions of the profile, separated by the dotted line, represent our estimation of the intensity fractions due to singlet $^1\Sigma^+$ (upper portion) and triplet $^3\pi$ (lower portion) $CH^+$ precursor ions.

beam. The value $I_2/I^\circ$ was observed to reach a limit of 0.12 at high Mg number densities, allowing the calculation of $\sigma_2/\sigma_1 = 4.5 \pm 0.5$ by eq 12c. These results may be understood by identifying the two ion species as the classical (12%) and bridged (88%) structures giving rise to the stable and dissociative components of the beam, respectively. The structure and stability of the ethyl radical and cation have been the subject of many investigations. EPR measurements indicate that the ground-state radical has the classical structure,[35] while photoelectron spectroscopy results suggested the ion had the bridged structure.[36] This was substantiated by photoion–photoelectron correlation measurements from which it was concluded that the structures of the radical and ion were different.[37] While early theoretical work favored a classical structure for the ion, more recent calculations predicted that the bridge structure would be more stable.[38]

The branching ratio $I_1/I_2$ was found to be independent of the process of $C_2H_5^+$ formation (electron impact or chemical ionization) under our high source pressure conditions, implying equilibration between the two forms. Thus for the reaction

$$C_2H_5^+ \text{ (bridged)} \rightleftharpoons C_2H_5^+ \text{ (classical)} \qquad (13)$$

the free energy change $\Delta G^\circ = 0.8 \pm 0.1$ kcal/mol can be calculated from the value of $K_{eq} = (1 - \alpha)/\alpha$ at a source temperature of 200 K. Since the entropy change for reaction 13 is expected to be positive, this value for $\Delta G^\circ$ serves as a lower limit for $\Delta H^\circ$. An upper limit to the barrier to 1,2 hydrogen migration in the classical radical of 2.2 eV is calculated from the fragmentation energy of the lowest state of the bridged radical observed.[39]

## Spin Isomers: $CH^+$

In some cases the structure of an ion depends on the ion source condition under which it was produced. Figure 5B illustrates CH neutral beam profiles from $CH^+$ ions obtained from electron impact on $He/CHCl_3$ mixtures.[20] These show a composite of two dissociative profiles for which the branching ratio is dependent on the pressure of He in the ion source, while the FE's are independent of source pressure. This indicates the presence of two distinguishable ions in the beam. An accurate electron impact appearance potential measurement[40] indicates that $CH^+$ is produced in a number of electronic states in the energy range above the appearance potential. Theoretical calculations by Green et al.[41] place the low-lying triplet state of $CH^+(^3\pi)$ 1.14 eV above the $^1\Sigma^+$ ground state. Since the residence time of $CH^+$ in our ion source (1–10 $\mu$s) is probably long enough for optical relaxation of the ion to occur by most allowed electronic transitions within the singlet or triplet manifold, we can assert that the $CH^+$ ions exiting the ion source are primarily in either the singlet ground state or the lowest triplet state.

Further consideration of the effect of He addition to the ion source allows the identification of the broad-base portion of the profile (FE = −3.95 eV) and the narrower central region (FE = −0.50 eV) with the $^3\pi$ and $^1\Sigma^+$ states of $CH^+$, respectively. As charge transfer to $He^+$ to produce $CH^+$ ($^3\pi$) is not energetically favorable,[42] the decreasing triplet to singlet ratio observed with increasing He pressure results from the increasing importance of $CH^+$ ($^1\Sigma^+$) production by charge transfer. The 3.45-eV difference in FE of the two processes is too great for the effect of He pressure in the ion source to be explained on the basis of vibrational relaxation of the ion. In addition vibrational excitation in the ion would lead to a distribution of FE's rather than the two widely separated values obtained. Further consideration based on the fragmentation energies and the energy levels of CH[43] allow the identification of the $^2\Sigma^+$ and $^4\pi$ states of CH as the products of electron transfer to the $^1\Sigma^+$ and $^3\pi$ states of $CH^+$, respectively. It is interesting to note that there is no need to invoke changes in orbital angular momentum to explain these results.

## Concluding Remarks

Perhaps the most significant technical advance from neutralized ion beam studies is the capability of pro-

(35) D. Griller, P. R. Marriot, and K. F. Preston, *J. Chem. Phys.*, **71**, 3703 (1979).
(36) F. A. Houle and J. L. Beauchamp, *J. Am. Chem. Soc.*, **101**, 4067 (1979).
(37) T. Baer, *J. Am. Chem. Soc.*, **102**, 2482 (1980).
(38) G. I. Gellene, N. S. Kleinrock, and R. F. Porter, *J. Chem. Phys.*, **78**, 1795 (1983) and references therein.
(39) The value of 2.2 eV is the sum of the calculated fragmentation energy of 0.5 eV and the dissociation energy of 1.7 eV for the ground-state ethyl radical from J. L. Franklin, J. G. Dillard, H. M. Rosenstock, J. T. Herron, and K. Draxel, *Natl. Bur. Stand. (U.S.) Arc.*, No. 26.
(40) J. D. Morrison and J. C. Traeger, *Int. J. Mass Spectrom. Ion Phys.*, 11, 289 (1973).
(41) S. Green, P. S. Bagus, B. Liu, A. D. McLean, and M. Yoshimine, *Phys. Rev. A*, **5**, 1614 (1972).
(42) H. M. Rosenstock, K. Draxl, B. W. Steiner, and J. T. Herron, *J. Phys. Chem. Ref. Data*, **6**, Suppl. 1 (1977).
(43) K. P. Huber and G. Herzberg, "Constants of Diatomic Molecules", Van Nostrand-Reinhold, New York, 1979.

ducing beams of stable or metastable molecules that would be difficult, if not impossible, to obtain by other methods. The potential to generate an essentially unlimited number of different neutral species can be an impetus for other experiments using beam techniques. In particular the technique may open up possibilities to obtain absorption spectra of metastables, using laser excitation with detection of photofragments. Beam studies using laser-excited alkali-metal target atoms[44] may provide information on Rydberg states of unstable molecules formed by resonant electron transfer. A possible example is the reaction

$$Na^*(3p,^2P) + NH_4^+ \rightarrow NH_4^* (3p,^2T_2) + Na^+ \quad (14)$$

The $^2T_2$ state of $NH_4$ may then radiate to the $^2A_1$ ground state or dissociate with conversion of internal energy to fragment kinetic energy.

In its present form the technique is limited in deriving structural information that may be contained in beam profiles. An interesting technical advance in beam detection is the development of an array detector (channel plate) by de Bruijn and Los,[45] using the time of flight coincidence method of Meierjohann and Vogler.[15] The increased resolution in beam profiles offered by their technique may reveal structural information masked by the isotropic scattering profile in $I(\theta)$.

*The $H_2^+/M$ study was done in collaboration with Prof. J. J. Leventhal and C. E. Burkhardt at the University of Missouri in St. Louis. We also with to acknowledge the contributions of Dr. Paul Curtis, Dr. Brian Williams, and Ms. Nancy Kleinrock. In addition we are grateful to the National Science Foundation for financial support through the Material Science Center (Grant GH-33637), Cornell University, and NSF Grant CHE-7909274.*

(44) V. S. Kushawaha, C. E. Burkhardt, and J. J. Leventhal, *Phys. Rev. Lett.*, **45**, 1686 (1980).
(45) D. P. de Bruijn and J. Los, *Rev. Sci. Instrum.*, **53**, 1020 (1982).

# The Barrier to Internal Rotation in Ethane

RUSSELL M. PITZER

*Department of Chemistry, The Ohio State University, Columbus, Ohio 43210*

*Received April 25, 1980 (Revised Manuscript Received December 14, 1982)*

Rotation about single bonds is discussed in many chemistry textbooks and has important consequences in molecular structure and dynamics.[1] Since ethane is the simplest molecule containing a carbon–carbon single bond, it is the prototype molecule for internal rotation in a large number of molecules and has therefore been the most frequently studied molecule in internal rotation studies.

The existence of a barrier to internal rotation in ethane was established in the 1930's, and in subsequent years the rotational barriers in a large number of molecules have been measured. The discussion of the origin of these barriers in terms of interactions between atoms or bonds began even before any experimental values had been obtained, and it is curious that even after a considerable number of rotational barriers had been measured, little progress had been made in understanding their origin. It was not until the 1960's, when moderate-sized (by the standards of the 1980's) digital computers could be applied to theoretical calculations, that firm conclusions could be drawn concerning the fundamental interactions involved.

During the later 1870's it was pointed out that the lack of rotational isomers of molecules such as $CH_2ClCH_2Cl$ meant that rotation about CC single bonds is practically free.[2] Subsequently there was some discussion as to whether a small hindering potential existed or not, but no evidence on this question was obtained for some time.[2]

In the 1930's difficulties were found in the statistical mechanical treatment of the thermodynamic data for ethane, and the existence of an internal rotation barrier was one of several suggestions as to the source of these difficulties. The discrepancies were resolved in 1936 by Kemp and Pitzer, who showed that the third law entropy of ethane, in combination with other thermodynamic data, required the existence of a barrier of approximately 3 kcal/mol.[3] In 1951 this method of determining rotational barriers was reviewed by Pitzer, and, on the basis of the available data, a revised value of 2.875 ± 0.125 kcal/mol was given for ethane.[4]

Since the 1930's a number of other methods of measuring rotational barriers have been developed, and these were reviewed by Wilson in 1959.[5] Microwave spectroscopy, one of the more extensively used techniques, is not directly applicable to ethane because the molecule lacks a dipole moment. By the use of infrared spectroscopic data, however, Smith was able to show in 1949 that the staggered conformation of ethane is the lower energy one,[6] as had been expected. A new value of the barrier itself was not obtained in this study because transitions between the internal rotation (torsional) energy levels in ethane are forbidden by infrared selection rules. Nevertheless, Weiss and Leroi, in 1968, were able to find these transitions by carrying out a

Russell M. Pitzer obtained his Bachelor's degree in 1959 from the California Institute of Technology, where he majored in chemistry and football. He did his graduate work with William N. Lipscomb at Harvard University, receiving a Ph.D. degree in chemical physics in 1963. His research interests concern electronic structure theory: the applications of it to organic biradicals and transition-metal complexes and the use of symmetry in it.

(1) W. G. Dauben and K. S. Pitzer in "Steric Effects in Organic Chemistry", M. S. Newman, Ed., Wiley, New York, 1956.
(2) W. J. Orville-Thomas in "Internal Rotation in Molecules", W. J. Orville-Thomas, Ed., Wiley, New York, 1974.
(3) J. D. Kemp and K. S. Pitzer, *J. Chem. Phys.*, **4**, 749 (1936); *J. Am. Chem. Soc.*, **59**, 276 (1937).
(4) K. S. Pitzer, *Discuss. Faraday Soc.*, **10**, 66 (1951).
(5) E. B. Wilson, Jr., *Adv. Chem. Phys.*, **2** 367 (1959); *Proc. Natl. Acad. Sci. U.S.A.*, **43**, 816 (1957). See also R. A. Pethrick and E. Wyn-Jones, *Q. Rev., Chem. Soc.*, **23**, 301 (1969).
(6) L. G. Smith, *J. Chem. Phys.*, **17**, 139 (1949).

0001-4842/83/0116-0207$01.50/0 